

# Kinematical transformations in amorphous selenium alloys used in xerography

S. O. KASAP, C. JUHASZ

*Solid State Research Group, Department of Electrical Engineering, Imperial College of Science and Technology, Exhibition Road, London SW7 2BT, UK*

Differential scanning calorimetric (DSC) studies were carried out on xerographic photoreceptor materials of amorphous selenium (a-Se), a-Se<sub>1-x</sub>Te<sub>x</sub> and a-Se:0.5 wt% As alloys with various amounts of chlorine doping. Glass transformation kinetics of bulk and vapour-deposited film samples were essentially identical indicating a similar amorphous structure for both forms. The glass transition temperature,  $T_g$ , in the a-Se<sub>1-x</sub>Te<sub>x</sub> system was found to increase monotonically with the tellurium content up to ~13 wt% which was accompanied by a fall in the activation energy,  $E_{gl}$ , for the structural relaxation. 0.5 wt% As increased  $T_g$ , whereas chlorine doping in the amounts used (~100 ppm) had no effect on  $T_g$ . Crystallization exotherms were analysed using the Kissinger method which was shown to remain a valid analysis by integrating the fundamental Kolmogoroff equation describing crystallization transformations by nucleation and growth. The significance of the activation energy,  $E_A$ , and the frequency factor,  $C_0$ , in the Kissinger analysis is discussed and used in interpreting the different crystallization behaviour exhibited by the various alloys. The apparent activation energy,  $E_A$ , of the crystallization kinetics was found to fall with the temperature range accessed in the DSC experiment. When other authors' previous crystallization studies by other methods were also considered, then  $1/E_A$  was found to fall nearly linearly with the mean reciprocal temperature,  $\langle 1/T \rangle$ , used in the experiment. It is argued that this behaviour arises if the crystal growth rate scales with the inverse viscosity of the melt and the latter is described by a Vogel–Tammann–Fulcher type of behaviour. The additives tellurium and arsenic retard the crystallization essentially by increasing the viscosity. Chlorine doping was also found to have an inhibitory effect but due probably to a change in the nucleation kinetics, rather than a viscosity rise.

## 1. Introduction

Amorphous selenium (a-Se) and its arsenic and tellurium alloys with various amounts of chlorine doping in the p.p.m. range are widely used in the fabrication of commercial xerographic photoreceptors in industry [1, 2]. Early photoreceptors employed the chlorine-doped a-Se<sub>0.995</sub>As<sub>0.005</sub> alloy rather than pure a-Se inasmuch as the latter was thermodynamically more unstable and tended to crystallize readily under typical machine operating conditions. The current trend in photoreceptor fabrication, however, is to use Se<sub>1-x</sub>Te<sub>x</sub> alloys with various amounts of chlorine doping [3]. Alloying with tellurium reduces the electronic bandgap and thus results in a photoreceptor having more desirable spectral response for xerographic purposes. For laser printer type of applications, the tellurium alloying may be as much as ~20 wt%. Although the Se:Te alloys are now widely used in the xerographic industry, there seems to be little available thermal characterization of these materials.

Several authors have recently investigated the glass transition [4–6] and crystallization phenomena [6–11] in bulk (vitreous selenium) and vapour-deposited a-Se using DTA. Matsuura and Suzuki [6], for example, reported identical glass transition behaviour for a-Se

samples prepared by melt quenching and vapour deposition, whereas their crystallization behaviour was distinctly different. The glass transition temperature,  $T_g$ , as obtained from DTA, has been found to depend on the heating rate [4, 6], ageing [4] and illumination [5]. The  $T_g$  data have been interpreted by a kinetic process based on structural relaxation concepts [12–14]. The relaxation time characterizing the structural enthalpy relaxation has been reported to have a thermal activation energy of ~2.47 eV atom<sup>-1</sup>.

The crystallization behaviour of a-Se has been found to depend on the preparation methods [6–8], nature of the substrates [9], impurities [15–17] and other factors [18]. Since the early models for the structure of a-Se were based primarily on a mixture of monomer ring molecules (Se<sub>8</sub> and others, e.g. Se<sub>6</sub> [19, 20]) and polymeric helical chain molecules, Se<sub>∞</sub>, most interpretations of the crystallization mechanism incorporated ring breaking (for which the energy is ~2 eV). The recent models [21, 22], however, indicate that the structure probably consists almost exclusively of selenium "chains" in which there may be ring-like regions (ring fragments). The latter regions occur where, along a few of the atoms in a chain, the dihedral angle alternates in sign. Ring fragments essentially cause chain bending. Although the chain

model for the structure of a-Se is supported by models for the vibrational spectra [23], the density of electronic states [24], and the radial distribution function (RDF) [25], the existence of Se<sub>8</sub> rings has not been completely ruled out.

## 2. Theory of non-isothermal crystallization kinetics

The fundamental phenomenological equation describing the evolution of the extended volume fraction,  $V_{\text{ex}}$ , with time in a crystallization phase transformation by nucleation and growth is the so-called Kolmogoroff equation [26]:

$$V_{\text{ex}}(t) = g \int_0^t I_v \left[ \int_{t'}^t u dt \right]^m dt' \quad (1)$$

where  $I_v$  is the nucleation rate per unit volume,  $u$  the growth rate,  $m$  the dimensionality of growth, and  $g$  a geometric factor determined by the morphology of growth. The fractional extended volume and the transformed volume fraction,  $X$ , are normally related by [27–30]

$$X = 1 - \exp(-V_{\text{ex}}) \quad (2)$$

As pointed out recently by a number of authors [31–36], any description of the crystallization kinetics must involve the integration of Equation 1. Under isothermal conditions and with certain assumptions on  $I_v$  and  $u$ , Equations 1 and 2 lead to the well known Johnson–Mehl–Avrami (JMA) equation (e.g. [37])

$$X = 1 - \exp(-Kt^n) \quad (3)$$

where  $K$  is the thermally activated rate constant and  $n$  the Avrami exponent. Equation 3 strictly applies under isothermal conditions and has as its theoretical basis the isothermal integration of Equation 1. Experimentally, many isothermal crystallization kinetics are well described by the JMA equation. Many authors [38–46], however, have used the JMA equation in developing thermal methods of analysis of crystallization exotherms observed in typical DTA experiments in which the conditions are non-isothermal, namely  $T = \beta t + T_0$  where  $\beta$  is the heating rate and  $T_0$  the initial temperature. There are at present a number of elaborate thermo-analytical methods developed from the incorrect use of Equation 3 when  $T = \beta t + T_0$ . For the purposes of this paper the Kissinger method [47, 48], which has been successfully applied to the study of crystallization kinetics of a variety of glasses [6, 9, 10, 49–53], is derived from the fundamental Equations 1 and 2. Originally this method was developed to study the kinetics of chemical reactions which are described by an  $n$ -order Eyring equation, i.e.

$$\dot{X} = (1 - X)^n C_0 \exp(-E_A/kT) \quad (4)$$

where  $C_0$  is the frequency factor.

In the following analysis it will be assumed that the growth velocity,  $u$ , can be simplified to

$$u = u_0 \exp(-E_G/kT) \quad (5)$$

where the activation energy  $E_G \gg kT$  in the experimental temperature range of interest.

## 2.1. Heterogeneous nucleation

If nucleation occurs from  $N$  number of heterogeneous sites and also very early in the transformation, then Equation 1 is essentially:

$$V_{\text{ex}}(t) = gN \left[ u_0 \int_0^t \exp(-E_G/kT) dt \right]^m; \\ T = \beta t + T_0 \quad (6)$$

This equation can be integrated by making certain analytical approximations based on  $E_G \gg kT$  [33–34]. Its occurrence is not unique to DTA as it also appears in the analysis of other similar types of temperature ramp experiments, for example in TSC measurements [54]. From Equation 6 we can therefore obtain the following approximation to  $X$  [36]

$$X(T) = 1 - \exp \left\{ - [gN(u_0 k/E_G \beta)^m T^{2m}] \right. \\ \left. \times \exp(-mE_G/kT) \right\} \quad (7)$$

The Kissinger method is based on examining the heating rate,  $\beta$ , dependence of the temperature,  $T_c$ , of the crystallization exotherm peak where  $d^2X/dt^2 = 0$ . Differentiating Equation 7 twice with respect to  $t$  (using  $dX/dt = \beta dX/dT$ ) and setting this to zero at  $T = T_c$  we obtain (for details see [36])

$$(\beta/T_c^2)^m = mgN (u_0 k/E_G)^m \exp(-mE_G/kT_c) \quad (8)$$

which means that the Kissinger method remains valid since

$$\ln(\beta/T_c^2) = -E_G/kT_c + \ln \{ [gNm]^{1/m} (u_0 k/E_G) \} \quad (9)$$

This should be compared with that derived from the Eyring equation

$$\ln(\beta/T_c^2) = -E_G/kT_c + \ln(C_0 k/E_G) \quad (10)$$

The frequency factor,  $C_0$ , in the Eyring equation hence corresponds to the expression  $(gNm u_0^m)^{1/m}$  in the case of crystallization kinetics.

## 2.2. Homogeneous nucleation

When the nucleation rate is non-zero during growth then the integration of Equation 1 requires a functional form to be assigned to  $I_v$ . The nucleation rate in solids is generally given by an expression of the form [55, 56]

$$I_v = A_1(T) \exp[-(\Delta G^* + \Delta G_A)/kT] \quad (11)$$

where  $\Delta G^*$  is the free-energy barrier to the formation of a nucleus (the thermodynamic barrier to nucleation),  $\Delta G_A$  is the activation free energy for a critical size nucleus to become stable (kinetic barrier to nucleation), and  $A_1$  is a weakly temperature dependent constant. There are, of course, more general expressions for the nucleation process which also include the interfacial strain energies involved in the nucleation process but these would unnecessarily complicate the mathematical analysis since the simplest approach in the present analysis is to take on Arrhenius behaviour for  $I_v$ ,

$$I_v = I_0 \exp(-E_N/kT) \quad (12)$$

Although this is an over-simplification of the nucleation kinetics, it will be approximately true over a

limited temperature range. The integration of Equation 1 then leads to [36]

$$X(T) = 1 - \exp \left\{ - (gI_0 u_0^m k / \beta^{m+1} \varepsilon) T^{2m+2} \right. \\ \left. \times \exp [-(E_N + mE_G)/kT] \right\} \quad (13)$$

where  $\varepsilon$  is a constant, in the units of energy, defined by

$$1/\varepsilon = \sum_{r=0}^m {}^m C_r / (E_N + rE_G) \quad (14)$$

where  ${}^m C_r$  is the binomial coefficient. As in heterogeneous nucleation, Equation 14 can be differentiated twice with respect to time (using  $dX/dt = \beta dX/dT$ ) and set to zero to find the  $\beta - T_c$  relationship. The result is

$$\ln (\beta/T_c^2) = - \frac{(E_N + mE_G)}{(m+1)kT_c} + \ln (gI_0 u_0^m k/\varepsilon)^{1/(m+1)} \quad (15)$$

which shows that the conventional Kissinger method remains, as in the case of heterogeneous nucleation, unmodified but the activation energy obtained from the slope of  $\ln (\beta/T_c^2)$  against  $1/T_c$  now represents some average activation energy,  $E_A$ , for the whole transformation, namely  $(E_N + mE_G)/(m+1)$ . In contrast to Equation 9, however, the dimensionality of growth,  $m$ , does affect the slope unless  $E_N \approx E_G$ .

It is instructive to point out that if the JMA equation is used as the starting point then, taking into account the temperature and hence time dependence of  $K$ , the Kissinger method can only be obtained if  $E_G/kT \ll 1$  [34, 35] which is, of course, an unrealistic situation inasmuch as in most crystallization transformations  $E_G/kT \gg 1$  (typically  $\sim 20$ ).

### 3. Experimental procedure

The samples used in DSC experiments were either in bulk (vitreous) or vacuum-evaporated film form. Vitreous pellets obtained from various well-known major xerographic selenium suppliers were used for bulk samples. In the text the prefix f or b is used to indicate film or bulk form and capital suffix letters A, B, C to indicate the various suppliers of selenium when there is a distinct difference in the thermal behaviour of their samples. The pure selenium pellets used were of xerographic grade; 99.999%. The impurity contents of the samples were determined by spark source mass spectrometer analysis and the quoted p.p.m. chlorine doping values are typically within  $\sim 50\%$ .

The photoreceptor films were prepared by vacuum evaporation ( $10^{-6}$  to  $10^{-5}$  torr) of vitreous pellets from long open stainless steel boats on to heated pre-oxidized aluminium drums which were rotated during fabrication to ensure uniform coating.

Fabrication of a-Se alloys by vacuum evaporation has already been widely described in literature by a number of authors [57–59]. X-ray diffraction studies showed no evidence of crystallinity in the samples prepared by the method used. Various compositions of  $\text{Se}_{1-x}\text{Te}_x$  were obtained by mixing the correct amounts by weight of pure selenium with portions of the prealloyed master batches. The maximum tellurium

concentration was  $\sim 10\%$  in the undoped Se:Te alloy. Sample thicknesses were typically  $\sim 50 \mu\text{m}$ . Scanning electron microprobe (SEM) was used to obtain the arsenic and tellurium compositions across the sample thickness. Owing to fractionation effects it was found that the substrate region was slightly deficient in tellurium content, whereas the top surface region was slightly richer in tellurium content. The quoted tellurium concentrations refer to the average level of tellurium in the “bulk” of the sample. After fabrication, the films were aged over several months during which the material achieved thermal and electrical stability [60–62]. In the ageing process it is believed that the glass structure relaxes towards its metastable liquid-like equilibrium state in which all the “structural” defects have equilibrated [62].

The DSC studies were carried out on a Dupont Differential Thermal Analyser, type 990, equipped with the DSC cell attachment [63] as described previously by others [9, 64]. The samples, which were typically  $\sim 20$  mg, were placed in small aluminium pans and then sealed. The films were stripped off their aluminium substrates before being placed in the pans. An empty pan was used as the reference. Most temperature readings from the thermograms required a small calibration correction. The tests were carried out from room temperature upwards. The maximum heating rate used was  $20^\circ \text{C min}^{-1}$ .

## 4. Results and discussion

### 4.1. General results

Figs. 1 to 3 show some typical DSC thermograms on bulk and film a-Se (Figs. 1 and 2) and on a-Se:Te film alloys with and without chlorine doping. The glass transition is exhibited as an endothermic peak rather than a change in the base line inasmuch as the samples were well annealed at room temperature,  $T_A$ , for many months so that the enthalpy of the system would have relaxed towards its metastable melt phase value,  $H_c(T_A)$  [4, 65]. As the heating rate is increased both the glass transition endotherm and the crystallization exotherm peak shift to higher temperatures as illustrated in Fig. 2. Notice that as the crystallization exotherms shift to higher temperatures, due to an increase in  $\beta$  or due to alloying effects (Fig. 3) they become broader which, within the framework of the Eyring equation, imply that either the activation energy,  $E_A$ , decreases or there is a fall in the frequency factor,  $C_0$  [66]. The following general observations are apparent and provide useful qualitative conclusions.

Bulk a-Se samples, even from the same supplier but different batches (e.g. b-A and b-A') can exhibit wide variations in their crystallization behaviour, whereas the film samples evince very similar crystallization peaks. Chlorine addition of  $\sim 40$  p.p.m. shifts the crystallization peak to higher temperatures which indicates the inhibitory effect of chlorine. Dilatometric studies have also suggested chlorine-induced reduction in the growth rate [16]. From Fig. 3 it is clear that tellurium alloying of a-Se also causes a shift in the crystallization exotherms to higher temperatures but the effect of using chlorine and tellurium in combination is not additive, i.e. the crystallization behaviour

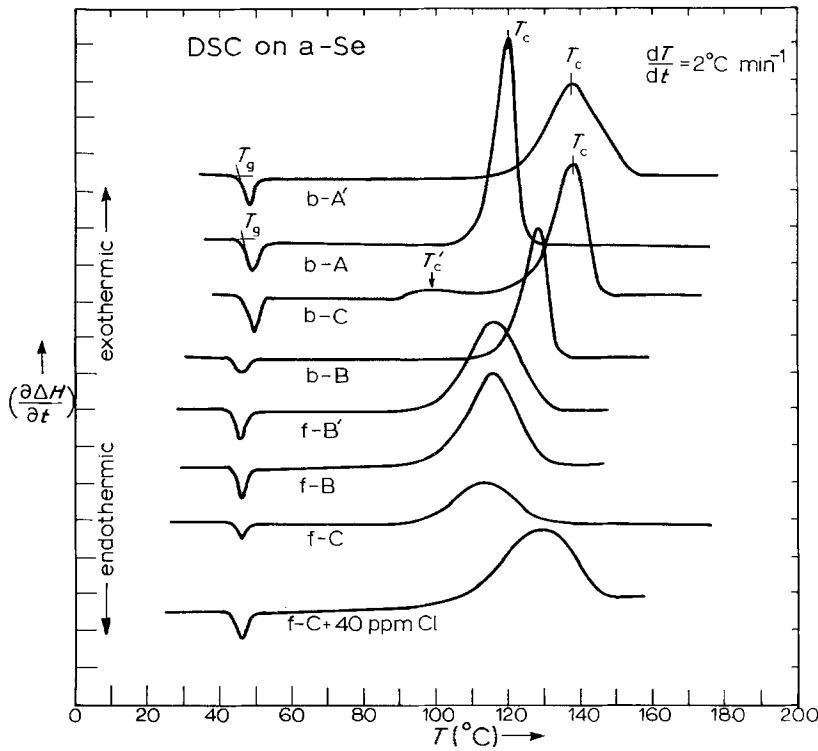


Figure 1 Some typical DSC thermograms of various types of a-Se (f, film; b, bulk) and  $\sim 40$  p.p.m. Cl-doped a-Se film. Heating rate  $\beta = 2^\circ\text{C min}^{-1}$ .

of chlorine-doped a-Se: Te alloy is very similar to both chlorine-doped selenium and a-Se:Te without chlorine.

Both film and bulk forms of a-Se evince similar  $T_g$  behaviour (Fig. 1) provided they have been sufficiently aged. Very recent samples showed lower values of  $T_g$ . At high heating rates (e.g.  $\beta = 20^\circ\text{C min}^{-1}$ )  $T_g$  for the heaviest bulk samples indicated 1 to  $2^\circ\text{C}$  larger  $T_g$  values which are not included in the following comparative analysis of the glass transition kinetics. It is apparent from Fig. 3 that alloying selenium with tellurium increases the glass transition temperature. Fig. 4 summarizes the dependence of the glass transition temperature and crystallization kinetics as characterized by  $T_0$  and  $T_c$  in a-Se: Te alloys on the tellurium composition.

#### 4.2. Glass transition

Fig. 5 shows semilogarithmic plots of the heating rate against the reciprocal glass transition temperature for film and bulk a-Se samples with and without chlorine-doping. It can be seen that the glass transition behaviour of various forms of a-Se with or without chlorine doping (up to 90 p.p.m.) are identical and the activation energy,  $E_{gl}$ , associated with the structural relaxation interpretation is 2.50 eV which is comparable with the values 2.47 and 2.58 eV reported by Matsuura and Suzuki [6], and Larmagnac *et al.* [4] respectively. In this kinetic interpretation, a structural property like the enthalpy  $H(T, t)$  (or the volume [67]) after an instantaneous isobaric change in the temperature is supposed to relax isothermally towards a new equilibrium value,  $H_c(T)$ , at that temperature via a

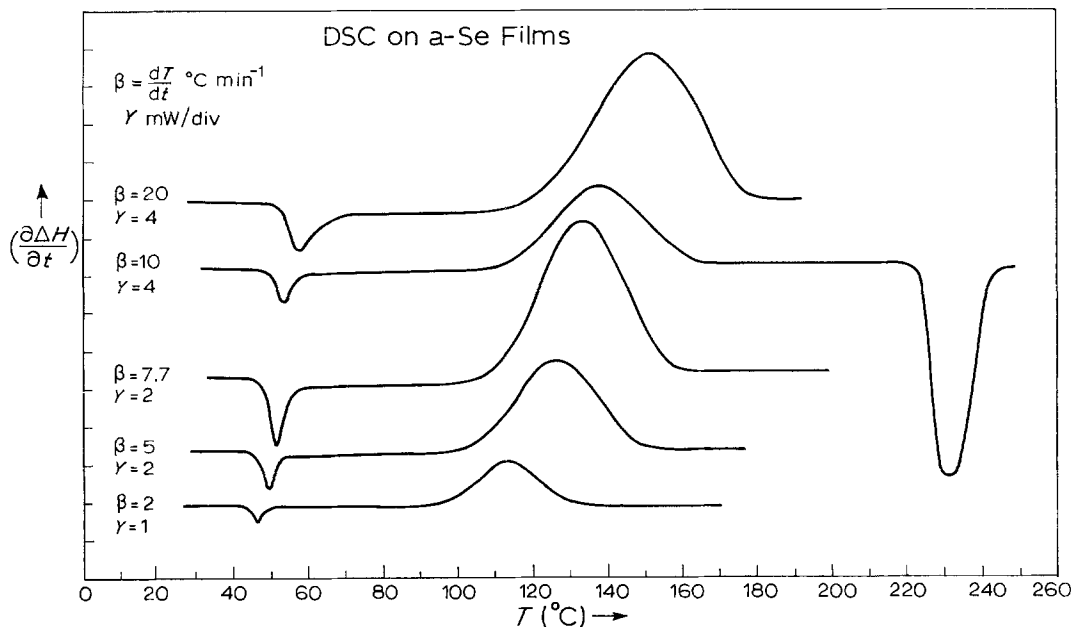


Figure 2 Typical DSC thermograms on a-Se films with the heating rate  $\beta$  varied from  $\beta = 2$  to  $20^\circ\text{C min}^{-1}$ .

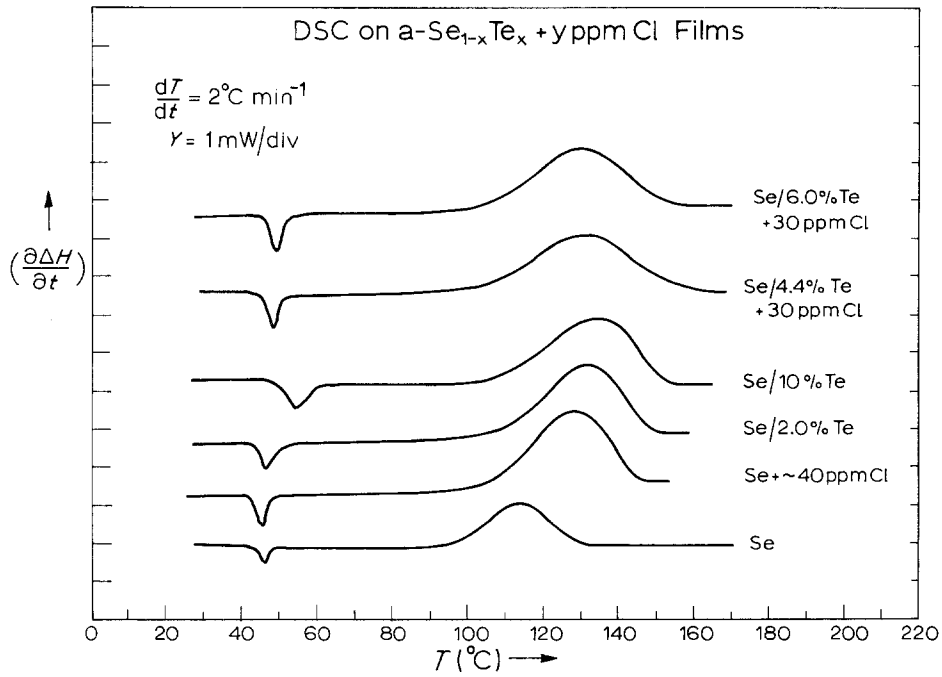


Figure 3 Typical DSC thermograms on a-Se<sub>1-x</sub>Te<sub>x</sub> films with various amount of Cl doping. Constant heating rate ( $\beta = 2^\circ\text{C min}^{-1}$ ).

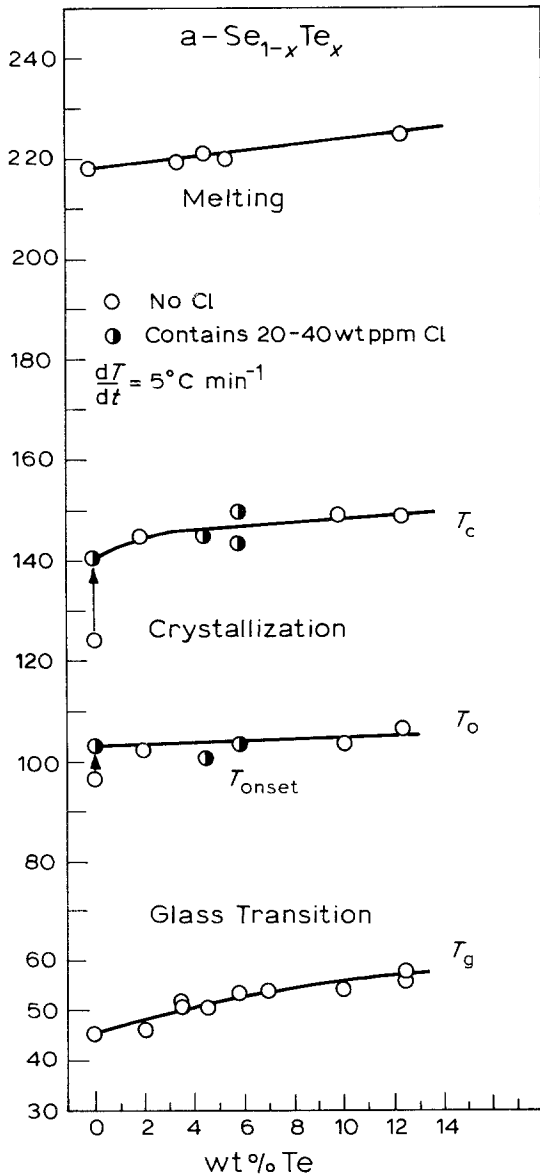


Figure 4 Summary of some DSC data on a-Se<sub>1-x</sub>Te<sub>x</sub> alloys showing the dependence of the glass transition, crystallization and melting behaviour on the tellurium composition.

relaxational equation of the form

$$(\partial H/\partial t)_T = -(H - H_e)/\tau(T) \quad (16)$$

where  $\tau$  is a temperature dependent structural relaxation time. Assuming, for example,  $\tau$  to be described by the equation

$$\tau = \tau_0 \exp(-E_{gl}/kT) \exp[-c(H - H_e)] \quad (17)$$

where  $\tau_0$  and  $c$  are constants, then it can be shown that [4, 12, 13]

$$\frac{d \ln \beta}{d(1/T_g)} = -E_{gl} \quad (18)$$

The slope of the  $\ln \beta$  against  $1/T_g$  plots, therefore, yields the activation energy involved in the molecular motions and rearrangements around  $T_g$ . Equation 18 is equivalent to the empirical relationship found by Bartenev and Lukianov [68]. Ritland derived it for  $T_g$  observed during cooling [69]. The expression for  $\tau$  in Equation 17 over a limited temperature range (as in DSC) is to a good approximation equivalent to those used by Moynihan *et al.* [12, 13], Ritland [69] and others [70, 71]. Note that the operational definition of  $T_g$  normally employed in DSC work is that temperature where the tangent at the inflection point of the glass transition endothermic peak intersects the base line. However, in an interpretation based on a glass to rubber phase transition with a rate determined by the Eyring theory, the temperature of the endothermic peak,  $T_{gm}$ , is of interest since its dependence on  $\beta$  then follows the Kissinger relationship [72]. We have not found as good a fit between the Kissinger relation and the experimental  $T_{gm}$  data as in the case of the  $\ln \beta$  against  $1/T_g$  analysis.

Fig. 6 shows the effect of tellurium and 0.5 wt % As addition to a-Se on the glass transformation kinetics. It is apparent that the  $\ln \beta$  against  $1/T_g$  plots move to higher temperatures with the tellurium content which is accompanied by a fall in  $E_{gl}$ . The rise in  $T_g$  with tellurium addition cannot thus be due to a change in

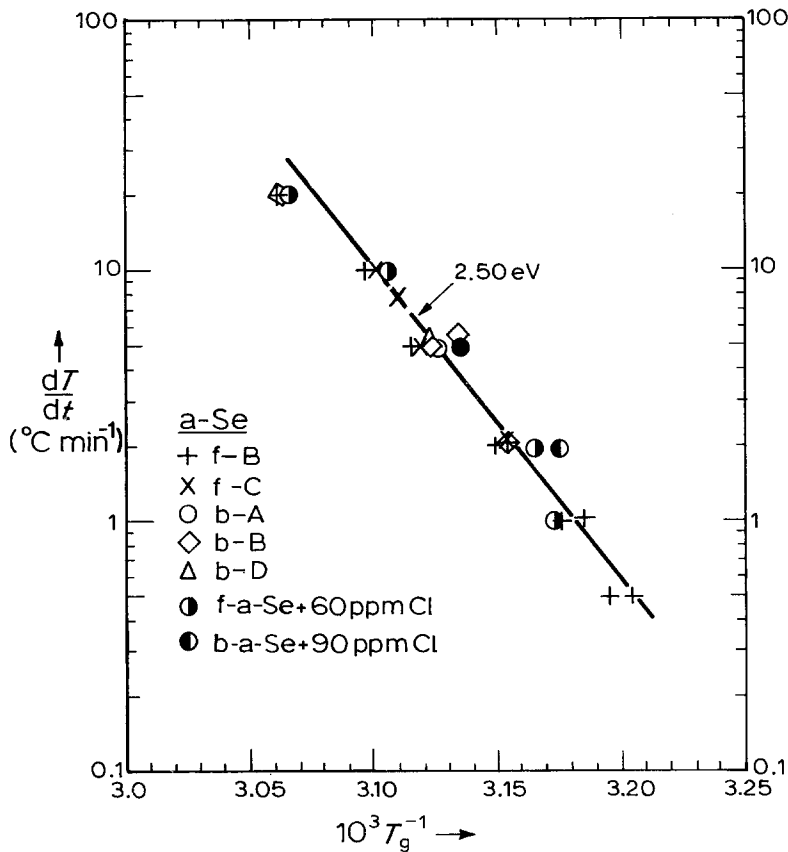


Figure 5 Semilogarithmic plot of the heating rate against the reciprocal glass transition temperature for various film and bulk a-Se samples.

the activation energy, but rather to a fall in the pre-exponential constant in Equation 17. The activation energy  $E_{gl} \approx 2.50 \text{ eV}$  for pure a-Se is larger than the Se-Se bond energy,  $1.91 \text{ eV}$ , which means that bond breaking during structural relaxation cannot be ruled out. Moreover, with tellurium addition,  $E_{gl}$  decreases (Fig. 6) which is consistent with the smaller Se-Te

bond energy ( $\sim 1.80 \text{ eV}$ ). However, it is doubtful that such significance can be attached to  $E_{gl}$ , as discussed later.

The monotonic increase in  $T_g$  with the tellurium content (Fig. 4) can be accounted for by an increase in the average molar mass,  $M_n$ , by the inclusion of heavier tellurium atoms in the polymeric chains

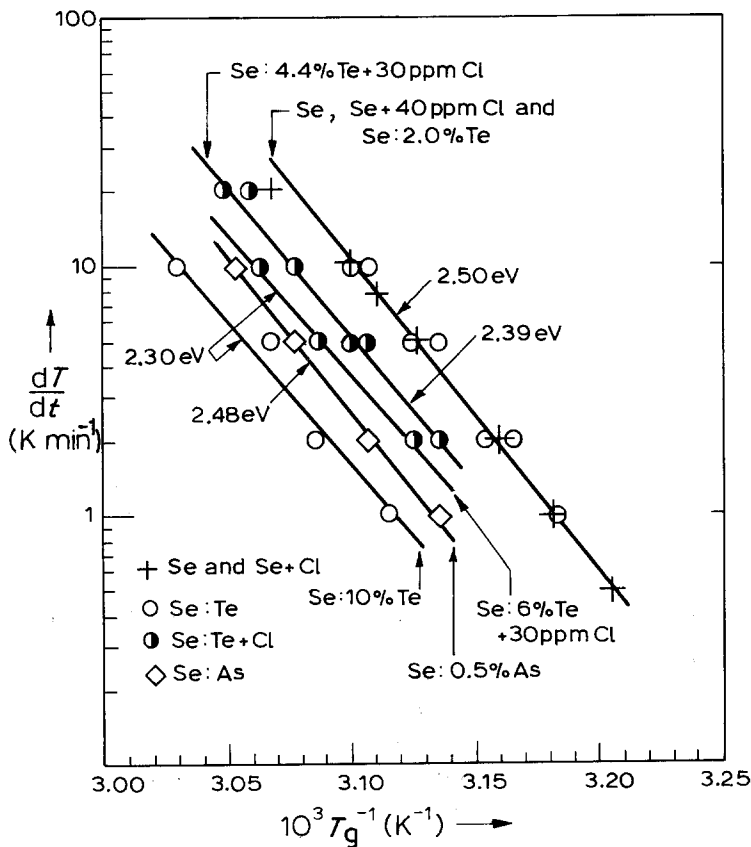


Figure 6 Semilogarithmic plot of the heating rate against the reciprocal glass transition temperature for a-Se<sub>1-x</sub>Te<sub>x</sub> film alloys and the 0.5 wt % As:Se bulk alloy.

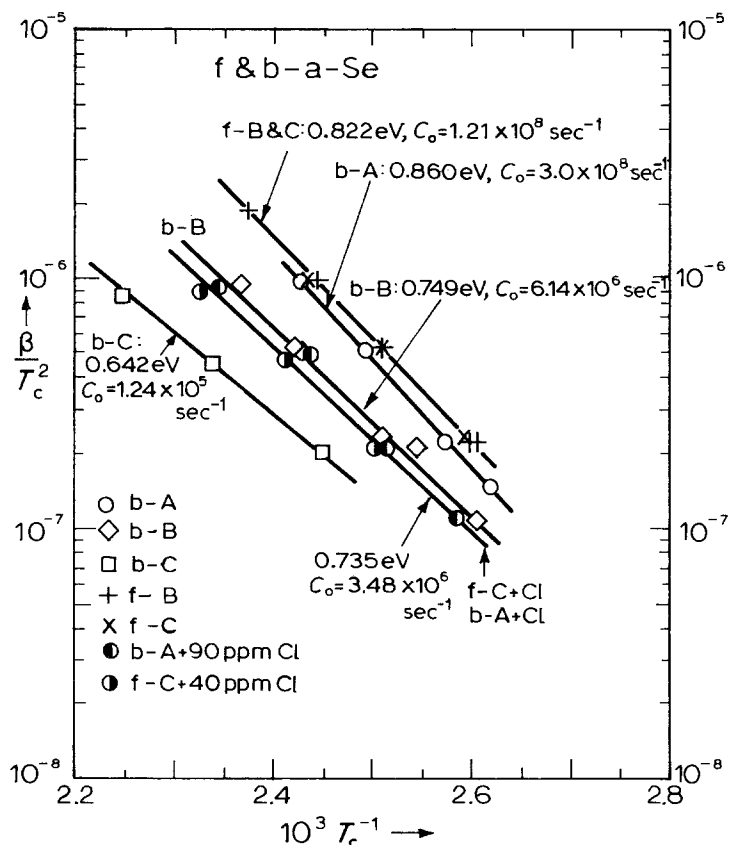


Figure 7 Kissinger plots of the crystallization kinetics in film and bulk a-Se samples. The associated frequency factors,  $C_0$ , are also shown.

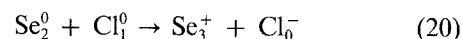
inasmuch as  $T_g$  depends on  $M_n$  via the well-known equation [73, 74] for polymers,

$$T_g = T_g^\infty - K_1 M_n^{-1} \quad (19)$$

where  $K_1$  is a constant and  $T_g^\infty$  is  $T_g$  at infinite molar mass. The observed copolymeric behaviour of the Se:Te alloys is in qualitative agreement with the recent studies on the structure of these alloys using neutron-diffraction techniques [75], which indicate that the freely rotating random chain model proposed for the structure of a-Se still persists up to large tellurium contents (70 at %) and that tellurium enters the structure essentially in a substitutional manner as predicted by the isoelectronic nature of the tellurium atom. In contrast, using dilatometry, Dzhililov and Rzaev [76] reported a linear decrease in  $T_g$  (observed during cooling) with tellurium content and interpreted the data as a decrease in  $M_n$ . It is instructive to note that if tellurium addition raises  $T_g$  (as in Fig. 4) then addition of sulphur should, by a similar argument, lower  $T_g$ , which has indeed been reported [77].

The higher  $T_g$  value for a-Se:0.5 wt % As (Fig. 6) can be attributed to the trivalent arsenic atoms cross-linking the selenium chains and thus forming a more rigid structure. It is interesting to note that chlorine addition in the amounts used showed no effect on the glass transition kinetics (Fig. 5) which is rather surprising since chlorine is well known as a selenium chain terminator [18, 78]. On this premise we would expect a fall in  $T_g$  with chlorine doping due to an increase in the free volume or, equivalently, a fall in  $M_n$  in Equation 19. Charge transport measurements by the present authors [79], however, suggest that chlorine addition also creates over-coordinated  $Se_3^+$  type of charged centres via the possible defect generat-

ing reaction



in which the number of bonds is conserved. The existence of over- and under-coordinated charged defect centres in chalcogenides, as proposed originally by Kastner, Mott and their co-workers [80–84], has been used in interpreting much of the data on electrical and optical properties of chalcogenides (e.g. [84–87]). Although chlorine addition may indeed reduce the average chain length, the cross-linking by  $Se_3^+$  centres from Equation 20 may be sufficient to counteract the implied fall in  $T_g$ . Further work on the effects of such defects on the thermal and mechanical properties of chalcogenides would obviously be useful. Note that the equivalent expression to Equation 19, which describes the effect of cross-linking on  $T_g$ , is [74]

$$T_g(\chi) = T_g(0) + K_2 \chi \quad (21)$$

where  $K_2$  is a constant and  $\chi$  is the number of cross-links per unit weight.

#### 4.3. Crystallization kinetics

It is evident from the various thermograms in Fig. 1 that the bulk a-Se samples display widely different crystallization behaviour. The films f-B and f-C, however, have exhibited identical crystallization kinetics which are distinctly different from those of the bulk parents. These observations are made clear by using Kissinger plots as shown in Fig. 7 where the activation energy and the frequency factor,  $C_0$ , of the transformations are also noted. The slopes yield the activation energy for growth,  $E_G$ , which seems to have lower values when the transformation occurs at higher temperatures. The  $C_0$  values vary between  $\sim 10^5$  (b-C)

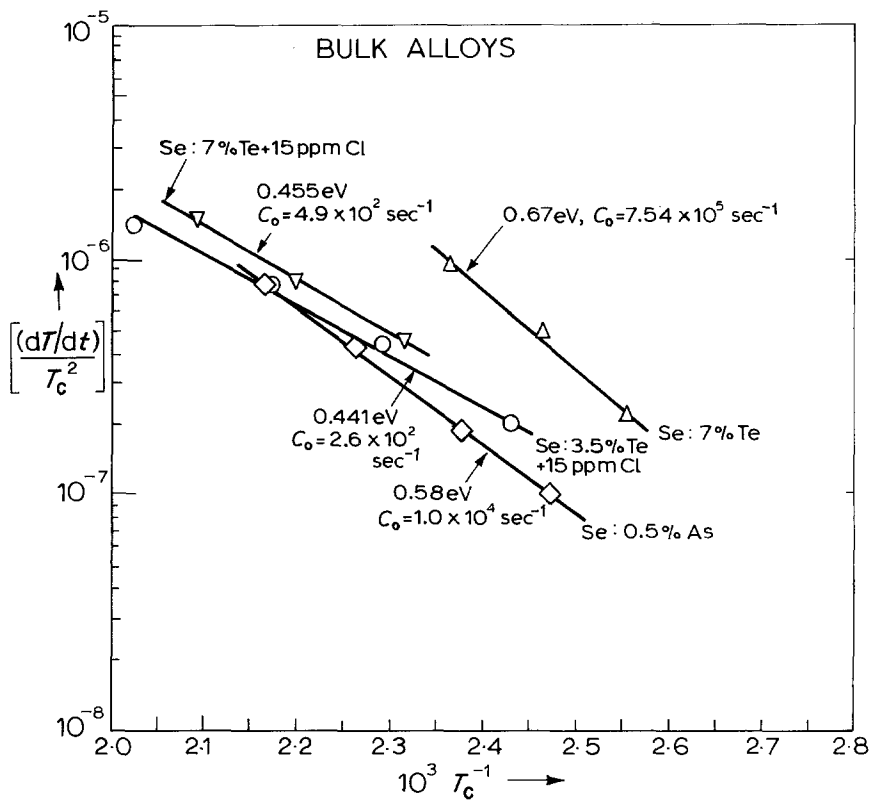


Figure 8 Kissinger plots of the crystallization kinetics in some a-Se:Te bulk alloys and the 0.5 wt % As:Se alloy.

and  $\sim 10^8$  (f-C) and, if interpreted via Equation 9, reflect differences in the nucleation site density,  $N$ , as well as in  $m$ , since in films growth is more likely to occur from the surface inwards [7, 8] ( $m = 1$  to 2), whereas in bulk samples we would also expect some bulk nucleation ( $m \sim 3$ ). Large variations in  $u_0$ , however, are unlikely since identical glass transition behaviour (Fig. 5) by all the selenium samples indicate very similar bulk structures suggesting similar amorphous-crystalline interface structures. The effect of

chlorine addition is also shown in Fig. 7, where the inhibitory action of chlorine on the crystallization kinetics is clearly apparent.

Figs. 8 and 9 display the Kissinger plots for bulk and film a-Se:Te alloys. It can be seen that tellurium alloying of a-Se causes the  $\ln \beta/T_c^2$  against  $1/T_c$  plots to shift to higher temperatures which is accompanied by a decrease in  $E_G$ . The crystallization kinetics for all the Se:Te films (with tellurium content from 2 to 10 wt %) with and without chlorine seems to be nearly

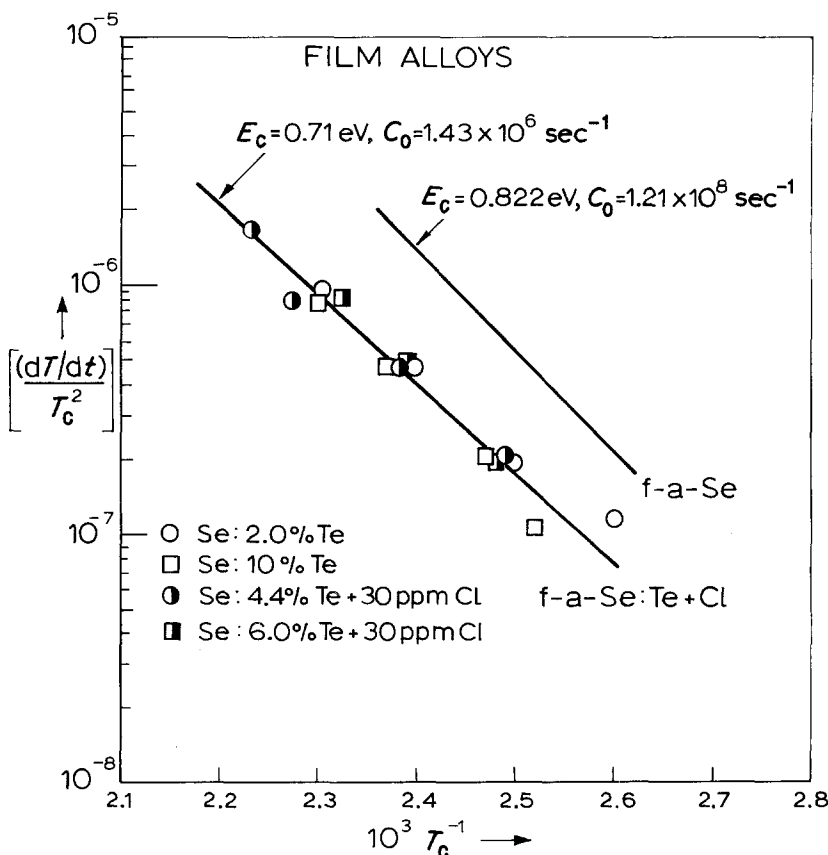


Figure 9 Kissinger plots of the crystallization kinetics in some a-Se:Te film alloys.



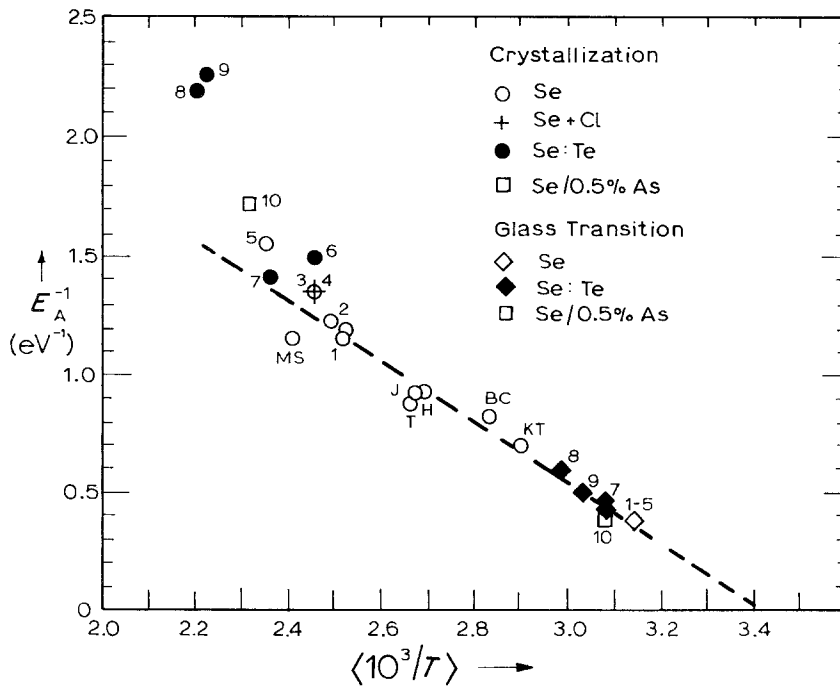


Figure 10 The dependence of the inverse activation energy of crystallization,  $1/E_A$ , on the mean reciprocal temperature  $\langle 1/T \rangle$  accessed in the experiment in this work (numbered 1 to 10) and in those using other experimental techniques (lettered). This work – selenium, (1) b-A; (2) f-B and C; (3) f-C + 40 p.p.m. Cl, b-A + 90 p.p.m. Cl; (4) b-B; (5) b-C; alloys, (6) b-7% Te; (7) f-4.5% Te + 26 p.p.m. Cl; (8) b-7% Te + 10 p.p.m. Cl; (9) b-3.5% Te + 15 p.p.m. Cl; (10) b-0.5% As. Other work – MS (Matsuura and Suzuki) [6]; T (Thornburg) [9]; H (Hamada *et al.*) [15]; BC (Brower and Capo) [105]; KT (Kim and Turnbull) [106]; J (Janjua *et al.*) [16].

identical, indicating comparable density of nucleation sites,  $N$ , and growth velocity constant,  $u_0$ , which is probably much slower than that for a-Se, since tellurium increases the average molecular weight. The bulk alloys displayed variations in their crystallization behaviour, tending to have lower  $E_G$  and  $C_0$  values, analogous to the case for bulk a-Se.

The most interesting feature of the  $\ln \beta/T_c^2$  against  $1/T_c$  plots in Figs. 7 to 9 is that the activation energy,  $E_A$ , decreases consistently and monotonically with the average temperature accessed during measurements. When  $1/E_A$  is plotted against  $\langle 1/T \rangle$  which is the average  $1/T$  for that particular experiment, we find the striking behaviour in Fig. 10 which also includes points from various authors' crystallization studies of a-Se by other experimental methods. Clearly the activation energy for the crystallization seems to obey the equation

$$(1/E_A) = (1/E_0) - (T_0/E_0)(1/T) \quad (22)$$

Moreover, as shown in Fig. 10, the activation energy values for the glass transformation,  $E_{gl}$ , for pure and tellurium alloyed a-Se also fall onto this line. If the crystallization kinetics is controlled by the viscous flow of the melt, then the trend in Fig. 10 is not unexpected if the viscosity has a Vogel–Tammann–Fulcher [88–91] (VTF) type of behaviour, i.e.

$$\eta = \eta_0 \exp [E_0/k(T - T_0)] \quad (23)$$

This viscosity relation, of course, implies a Williams–Landel–Ferry (WLF) [92–95] type of response in the mechanical and electrical relaxational process around  $T_g$ . The fact that WLF behaviour for the dielectric properties has been reported for a-Se near  $T_g$  [96] supports the assertion here that the growth kinetics of crystallization is limited by the viscosity of the amorphous phase. Further, WLF behaviour follows naturally from the free volume theories for  $T_g$  [97, 98] which means that the apparent activation energy,  $E_{gl}$ , has little significance in terms of intramolecular forces.

The deviation of data from Equation 22 in the high-temperature range is not unusual and is typical of amorphous structures which exhibit a VTF behaviour [99, 100]. For example, in a- $\text{As}_2\text{Se}_3$  [101], which is another commercially important xerographic amorphous semiconductor but with a higher  $T_g$ ,  $\sim 177^\circ\text{C}$ , the VTF behaviour observed around  $T_g$  fails above  $\sim 253^\circ\text{C}$ .

The lack of viscosity data on the amorphous phase around the crystallization temperatures (due to the obvious difficulties in the measurement) does not allow direct comparison between  $E_G$  and the apparent activation energy for the viscous flow,  $E_\eta$ . The viscosity–temperature experiments of Cukiermann and Uhlmann [102], however, when interpolated into the typical temperatures ranged in crystallization studies of a-Se, indicate a decrease in  $E_\eta$  with  $T$  with a high-temperature limit of  $\sim 0.75\text{ eV atom}^{-1}$  and an Arrhenian behaviour above  $\sim 200^\circ\text{C}$ . Considering the crudeness of Fig. 10 and increased errors in the Kissinger analysis as  $E_G/kT \gg 1$  holds less vigorously with  $T$  increasing, the behaviour of  $E_\eta$  and  $E_G$  probably compare well to assert that the growth kinetics is inversely proportional to the viscosity of the melt. Tellurium-induced retardation in the crystallization velocity is thus due to a viscosity increase which is consistent with the rise in  $T_g$ . Chlorine-induced retardation, in this interpretation, must be due to a change in the nucleation site density or in the nucleation kinetics since chlorine has no observable effect on  $T_g$ . Notice that in films of a-Se:Te (Fig. 9), chlorine has relatively no effect on the crystallization kinetics; the transformation velocity is limited mainly by the effect of the tellurium atoms.

Fig. 11 shows the dependence of the frequency factor  $C_0 = (gNm)^{1/m}u_0$  on tellurium composition.  $C_0$  seems to fall rapidly even with small additions of tellurium and saturates around  $\sim 10^6$  ( $\sim 10^3$  for some bulk samples). The fall in  $C_0$  by  $\sim 10^2$ , which compares well with the similar fall observed by Kim and

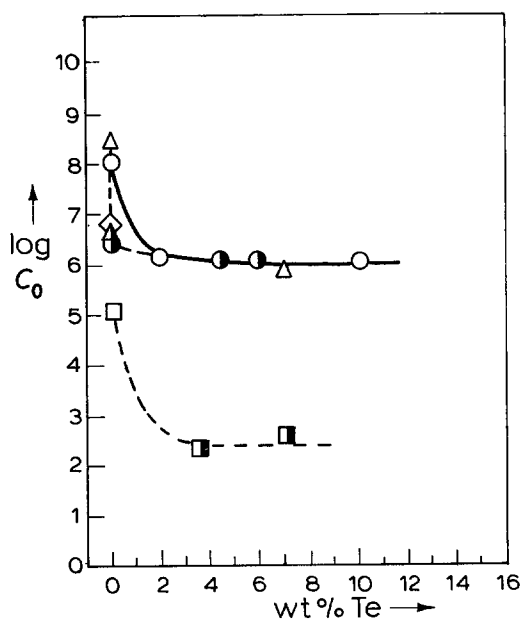


Figure 11 The dependence of the frequency factor,  $C_0$ , on the tellurium content. ○, film; △, b-A; ◇, b-B; □, b-C.

Turnbull [17] on the isothermal growth rates with tellurium addition, indicates a tellurium-induced reduction in  $u_0$ , i.e. an increase in  $\eta_0$  in Equation 21 since we proposed  $u \sim \eta^{-1}$ . Thus, the density of nucleation sites,  $N$ , probably remains relatively unaffected by tellurium addition. Some of the bulk Se:Te samples, however, have shown a larger fall in  $C_0$  (by  $\sim 10^3$ ) which suggests a possible change in the nucleation kinetics, from heterogeneous to homogeneous (or a mixture), since orders of magnitude change in  $N$  are unlikely with introduction of a few atomic per cent tellurium. A change in the nucleation behaviour may also explain, via Equation 15, the fact that these alloys evince rather low slopes in their Kissinger plots (Fig. 8).

The inhibitory effect of 0.5 wt % As addition on the crystallization kinetics of a-Se (Fig. 8) can be accounted as for tellurium alloying, by an increased viscosity of the melt as discussed in Section 4.2.

## 5. Conclusions

Using the fundamental Kolmogoroff equation, the Kissinger method of thermal analysis is shown to remain valid without any essential modification for studying crystallization kinetics by nucleation and growth. The significance of the activation energy,  $E_A$ , and the frequency factor,  $C_0$ , determined via this thermoanalytical method has been shown to depend on the nucleation kinetics and is discussed in the text.

Glass transition kinetics of all the bulk and film a-Se samples, once aged, were identical suggesting similar amorphous structures. This conclusion is further supported by the fact that the infrared [103] spectrum for a-Se samples quenched from liquids equilibrated at different temperatures evinces identical absorption features as discussed in detail by Lukovsky [21]. Moreover, the Raman spectrum also shows a similar behaviour [104].

Alloying of a-Se with tellurium up to  $\sim 12$  wt %, monotonically increases the glass transition tempera-

ture which is accompanied by a fall in the activation energy,  $E_{gl}$ , for the structural relaxation. Chlorine addition in the amounts used ( $\sim 100$  p.p.m.) has no effect on  $T_g$ . Introduction of 0.5 wt % As, however, raised  $T_g$ .

The additives tellurium (up to  $\sim 10$  wt %), arsenic (0.5 wt %) and chlorine (up to 100 p.p.m.) have been found to retard crystallization. The activation energy for growth,  $E_G$ , has been found to fall monotonically with temperature. When the crystallization studies of a number of other authors are also considered,  $1/E_A$  is shown to fall nearly linearly with  $\langle 1/T \rangle$ , the average  $1/T$  accessed during a particular experiment. This behaviour indicates that the growth velocity scales with the inverse viscosity,  $\eta$ , of the melt which is most likely described by a Vogel relation. Tellurium alloying thus increases the viscosity (by  $\sim 10^2$ ) but has relatively little effect on the density of nucleation sites. Arsenic also retards crystallization by raising the viscosity. The inhibitory effect of chlorine addition, however, cannot be accounted for by a change in the viscosity, and the inhibitory mechanism therefore remains unresolved.

Although the film samples have identical crystallization kinetics the bulk samples have shown widely differing behaviour and tended to give various lower  $C_0$  values due either to bulk crystallization or a mixture of nucleation kinetics. Both in bulk and film samples the crystallization velocity is controlled by the viscous flow in the melt.

Amorphous selenium and Se:Te alloys portray typical glassy polymeric and copolymeric behaviour.

## Acknowledgements

It is a pleasure to acknowledge the helpful assistance of Mr R. N. Shephard of the Department of Chemistry, Imperial College. We wish to thank Mr J. R. Hardwick of Gestetner (Byfleet) Ltd, UK for financial support and Drs R. Rollason and J. Turner also of Gestetner (Byfleet) Ltd for many useful suggestions.

## References

1. S. B. BERGER, R. C. ENCK, M. E. SCHARFE and B. E. SPRINGETT, in "Physics of Selenium and Tellurium", edited by E. Gerlach and P. Grosse (Springer-Verlag, New York, 1979) pp. 256–267.
2. L. CHEUNG, G. M. T. FOLEY, P. FOURNIA and B. E. SPRINGETT, *Photogr. Sci. Eng.* **26** (1982) 245.
3. C. JUHASZ, M. VAEZI-NEJAD and S. O. KASAP, *J. Im. Sci. (Photogr. Sci. Eng.)* **29** (1985) 144.
4. J. P. LARMAGNAC, J. GRENET and P. MICHON, *J. Non-Cryst. Solids* **45** (1981) 157.
5. *Idem*, *Phil. Mag. B* **45** (1982) 627.
6. M. MATSUURA and K. SUZUKI, *J. Mater. Sci.* **14** (1979) 395.
7. M. KAWARADA and Y. NISHINA, *Jpn. J. Appl. Phys.* **16** (1977) 1525.
8. *Idem*, *ibid.* **16** (1977) 1531.
9. D. D. THORNBURG, *Thin Solid Films* **37** (1976) 215.
10. J. GRENET, J. P. LARMAGNAC and P. MICHON, *ibid.* **67** (1980) L17.
11. E. A. MARSEGLIA and E. A. DAVIES, *J. Non-Cryst. Solids* **50** (1982) 13.
12. C. T. MOYNIHAN, A. J. EASTEAL, J. WILDER and J. TUCKER, *J. Phys. Chem.* **78** (1974) 2673.
13. C. T. MOYNIHAN, A. J. EASTEAL and M. A. DE BOLT, *J. Amer. Ceram. Soc.* **59** (1976) 12.

14. M. A. DE BOLT, A. J. EASTEAL, P. B. MACEDO and C. T. MOYNIHAN, *ibid.* **59** (1976) 16.
15. S. HAMADA, T. SATO and T. SHIRAI, *Bull. Chem. Soc. Jpn.* **40** (1967) 864.
16. M. B. I. JANJUA, J. M. TOGURI and W. C. COOPER, *Can. J. Phys.* **49** (1971) 475.
17. K. S. KIM and D. TURNBULL, *J. Appl. Phys.* **45** (1974) 3447.
18. W. C. COOPER and R. A. WESTBURY, in "Selenium", edited by R. A. Zingaro and W. C. Cooper (Van Nostrand Reinhold, New York, 1974) Ch. 3, pp. 87-148 and references therein.
19. H. RICHTER and F. HERRE, *Z. Naturforsch.* **13a** (1958) 847.
20. N. J. SHEVCHIK, *Phys. Rev. Lett.* **33** (1974) 1572.
21. G. LUKOVSKY, in "Physics of Selenium and Tellurium" edited by E. Garlach and P. Grosse (Springer-Verlag, New York, 1979) p. 178.
22. G. LUKOVSKY, F. L. GALEENER, *J. Non-Cryst. Solids* **35-36** (1980) 1209 and references therein.
23. P. E. MEEK, *Phil. Mag.* **34** (1976) 767.
24. J. ROBERTSON, *ibid.* **34** (1976) 13.
25. M. LONG, P. GALLISON, R. ALBEN and G. CONNELL, *Phys. Rev. B* **13** (1976) 1821.
26. A. N. KOLMOGOROV, *Izv. Ak. Nauk. SSSR Ser. Matematicheskaya* **1** (1937) 355.
27. M. AVRAMI, *J. Chem. Phys.* **7** (1939) 1103.
28. *Idem*, *ibid.* **8** (1940) 212.
29. *Idem*, *ibid.* **9** (1941) 177.
30. W. A. JOHNSON and R. F. MEHL, *Trans. Amer. Min. Met. Eng.* **135** (1939) 416.
31. D. W. HENDERSON, *J. Non-Cryst. Solids* **30** (1979) 301.
32. *Idem*, *J. Thermal Anal.* **15** (1979) 325.
33. T. J. W. DE BRUIJN, W. A. DE JONG and P. J. VAN DER BERG, *Thermochim. Acta* **45** (1981) 315.
34. H. YINNON and D. R. UHLMANN, *J. Non-Cryst. Solids* **54** (1983) 253.
35. D. R. UHLMANN and H. YINNON, in "Glass: Science and Technology", edited by D. R. Uhlmann and N. J. Kreidl, Vol. 1 (Academic Press, New York, 1983).
36. S. O. KASAP and C. JUHASZ, *J. Chem. Soc. Faraday Trans.* **81** (1985) 811.
37. J. W. CHRISTIAN, "The Theory of Transformations in Metals and Alloys", 2nd Edn, Part 1 (Pergamon Press, Oxford, 1985) Chs. 1 and 2.
38. R. L. THAKUR and S. THIAGARAJAN, *Bull. Central Glass Ceram. Res. Inst. (Salcutta)* **15**(3) (1968) 67.
39. R. L. THAKUR, in "Advances in Nucleation and Crystallization of Glasses", edited by L. L. Hencht and S. W. Freiman, 73rd Annual Meeting, American Ceramic Society (American Ceramic Society, Columbus, Ohio, 1971) pp. 166-72.
40. J. A. AUGIS and J. E. BENNETT, *J. Thermal Anal.* **13** (1978) 283.
41. E. A. MARSEGLIA, *J. Non-Cryst. Solids* **41** (1980) 31.
42. K. HARNISCH and R. LANZENBERGER, *ibid.* **53** (1982) 235.
43. A. MAROTTA, S. SCIELLO and A. BURI, *ibid.* **57** (1983) 473.
44. M. R. KAMAL and E. CHU, *Polymer Eng. Sci.* **23** (1983) 27.
45. S. SURINACH, M. D. BARO, M. T. CLAVAGUERA-MORA and N. CLAVAGUERA, *J. Non-Cryst. Solids* **58** (1983) 209.
46. P. MICHON, H. ATMANI and C. VAUTIER, *Phys. Status Solidi A* **85** (1984) 399.
47. H. E. KISSINGER, *J. Res. Nat. Bur. Stand.* **57** (1956) 217.
48. *Idem*, *Anal. Chem.* **29** (1957) 1702.
49. S. RISBUD, *J. Amer. Ceram. Soc.* **56** (1973) 440.
50. P. G. BOSWELL, *Scripta Metall.* **11** (1977) 701.
51. *Idem*, *J. Mater. Sci.* **15** (1980) 1926.
52. K. MATUSITA and S. SAKKA, *J. Non-Cryst. Solids* **38-39** (1980) 741.
53. R. FRAHM, *ibid.* **56** (1983) 255.
54. R. CHEN, *J. Mater. Sci.* **11** (1976) 1521 and references therein.
55. J. H. HOLLOWMAN and D. TURBHULL, *Prog. Metal. Phys.* **4** (1935) 333.
56. D. TURNBULL, *Solid State Phys.* **3** (1956) 225.
57. J. S. BERKES, in "Electrophotography Second International Conference", Washington, DC, 1974, edited by D. R. White, (Society of Photographic Scientists and Engineers, Springfield, VA) pp. 137-141.
58. J. C. SCHOTTMILLER, *J. Vac. Sci. Technol.* **12** (1975) 807.
59. M. D. TABAK and W. J. HILLEGAS, *ibid.* **9** (1972) 387.
60. G. C. DAS, M. B. BEVER, D. R. UHLMANN and S. C. MOSS, *J. Non-Cryst. Solids* **7** (1972) 251.
61. R. B. STEPHENS, *ibid.* **20** (1976) 75.
62. M. ABKOWITZ, *Polymer Eng. Sci.* **24** (1984) 1149.
63. R. C. MACKENZI and B. D. MITCHELL, in "Thermal Analysis", Vol. 1, edited by R. C. Mackenzi (Academic Press, London, 1970) Ch. 3.
64. D. D. THORNBURG and R. I. JOHNSON, *J. Non-Cryst. Solids* **17** (1975) 2.
65. R. B. STEPHENS, *J. Appl. Phys.* **49** (1978) 5855.
66. R. L. REED, L. WEBER and B. S. GOTTFRIED, *I. and E.C. Fundamentals* **4** (1965) 38.
67. A. J. KOVACS, *Adv. Polym. Sci.* **4** (1963) 394.
68. G. M. BARTENEV and I. A. LUKIANOV, *Zh. Fiz. Khim.* **29** (1955) 1486.
69. H. N. RITLAND, *J. Amer. Ceram. Soc.* **37** (1954) 370.
70. Yu. A. SHARONOV and M. V. VOLKENSHTEIN, *Sov. Phys. Solid State* **6** (1964) 992.
71. O. S. NARAYANASWAMY, *J. Amer. Ceram. Soc.* **54** (1971) 491.
72. J. A. McMILLAN, *J. Chem. Phys.* **42** (1965) 3497.
73. T. G. FOX and P. J. FLORY, *J. Polym. Sci.* **14** (1954) 315.
74. T. G. FOX and S. LOSHAEK, *ibid.* **15** (1955) 371.
75. R. BELLISENT and G. TOURAND, *J. Non-Cryst. Solids* **35-36** (1980) 1221.
76. S. U. DZHALILOV and K. I. RZAEV, *Phys. Status Solidi* **20** (1967) 261.
77. M. B. MYERS and E. J. FELTY, *Mater. Res. Bull.* **2** (1967) 535.
78. T. SHIRAI, S. HAMADA and K. KOBAYASHI, *Nippon Kagaku Zasshi* **84** (1963) 968.
79. S. O. KASAP and C. JUHASZ, *J. Phys. D Appl. Phys.* **18** (1985) 703.
80. M. KASTNER, D. ADLER and H. FRITZSCHE, *Phys. Rev. Lett.* **37** (1976) 1504.
81. M. KASTNER, *J. Non-Cryst. Solids* **31** (1978) 223.
82. R. A. STREET and N. F. MOTT, *Phys. Rev. Lett.* **35** (1975) 1293.
83. N. F. MOTT, E. A. DAVIS and R. A. STREET, *Phil. Mag.* **32** (1975) 961.
84. "Electronic Processes in Non-Crystalline Materials", 2nd Edn. (Clarendon Press, Oxford, 1979) Ch. 9.
85. D. ADLER and E. J. YOFFA, *Can. J. Chem.* **55** (1977) 1920.
86. S. R. OVSHINSKY and D. ADLER, *Contemp. Phys.* **19** (1978) 109.
87. J. ROBERTSON, *Phys. Chem. Glasses* **23** (1982) 1 and references therein.
88. H. VOGEL, *Physik Z.* **22** (1921) 645.
89. G. TAMMANN and N. HESSE, *Z. Anorg. Chem.* **156** (1926) 245.
90. G. TAMMANN and A. ELBRACHTER, *ibid.* **207** (1932) 268.
91. H. FULCHER, *J. Amer. Ceram. Soc.* **8** (1925) 339.
92. M. L. WILLIAMS, F. R. LANDEL and J. D. FERRY, *J. Amer. Chem. Soc.* **77** (1955) 370.
93. M. L. WILLIAMS, *J. Phys. Chem.* **59** (1955) 95.
94. J. D. FERRY, "Viscoelastic Properties of Polymers", (Wiley, New York, 1980) Ch. 11.
95. G. E. ROBERTS and E. F. T. WHITE, in "The Physics of Glassy Polymers", edited by R. N. Haward (Applied Science, London, 1973) Ch. 3, p. 153 and references therein.
96. M. ABKOWITZ, D. F. POCHAN and J. M. POCHAN, *J. Appl. Phys.* **51** (1980) 1539.

97. M. H. COHEN and D. TURNBULL, *J. Chem. Phys.* **31** (1959) 1164.
98. D. TURNBULL and B. G. BAGLEY, in "Treatise on Solid State Chemistry", Vol. 5, Changes of States, edited by N. B. Hannay (Plenum, New York, 1975) Ch. 10 and references therein.
99. G. C. BERRY and T. G. FOX, *Adv. Polym. Sci.* **5** (1968) 261.
100. M. CUKIERMANN, J. W. LANE and D. R. UHLMANN, *J. Chem. Phys.* **59** (1973) 3639.
101. D. W. HENDERSON and D. G. AST, *J. Non-Cryst. Solids* **64** (1984) 43.
102. M. CUKIERMANN and D. R. UHLMANN, *ibid.* **12** (1973) 199.
103. R. C. KEEZER, G. LUKOVSKY and R. M. MARTIN, *Bull. Amer. Phys. Soc.* **20** (1975) 323.
104. M. H. BRODSKY, R. J. GAMBINO, J. E. SMITH and Y. YACOBY, *Phys. Status Solidi A* **52** (1972) 609.
105. W. F. BROWER and D. J. CAPO, *J. Vac. Sci. Technol.* **13** (1976) 1066.
106. K. S. KIM and D. TURNBULL, *J. Appl. Phys.* **44** (1973) 5237.

*Received 30 April  
and accepted 12 June 1985*